

Dear Author

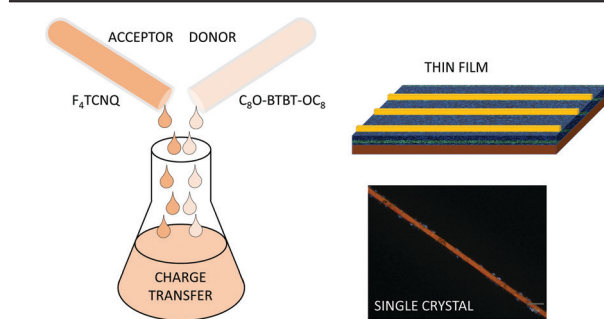
Please use this PDF proof to check the layout of your article. If you would like any changes to be made to the layout, you can leave instructions in the online proofing interface. First, return to the online proofing interface by clicking "Edit" at the top of the page, then insert a Comment in the relevant location. Making your changes directly in the online proofing interface is the quickest, easiest way to correct and submit your proof.

Please note that changes made to the article in the online proofing interface will be added to the article before publication, but are not reflected in this PDF proof.

If you would prefer to submit your corrections by annotating the PDF proof, please download and submit an annotatable PDF proof by clicking the button below.

 [Annotate PDF](#)

We have presented the graphical abstract image and text for your article below. This briefly summarises your work, and will be presented with your article online.



Charge transfer complexes of a benzothienobenzothiophene derivative and their implementation as active layer in solution-processed thin film organic field-effect transistors

Lamiaa Fijahi, Tommaso Salzillo,* Adrián Tamayo, Marco Bardini, Christian Ruzié, Claudio Quarti, David Beljonne,* Simone d'Agostino,* Yves Geerts and Marta Mas-Torrent*

Single crystals of novel $(C_8O-BTBT-OC_8)(F_xTCNQ)$ charge complexes (CT) are prepared and fully characterised. Solution processed films of the $(C_8O-BTBT-OC_8)(F_4TCNQ)$ CT are implemented in organic field-effect transistors giving an n-type behaviour.

Please check this proof carefully. Our staff will not read it in detail after you have returned it.

Please send your corrections either as a copy of the proof PDF with electronic notes attached or as a list of corrections. **Do not edit the text within the PDF or send a revised manuscript** as we will not be able to apply your corrections. Corrections at this stage should be minor and not involve extensive changes.

Proof corrections must be returned as a single set of corrections, approved by all co-authors. No further corrections can be made after you have submitted your proof corrections as we will publish your article online as soon as possible after they are received.

Please ensure that:

- The spelling and format of all author names and affiliations are checked carefully. You can check how we have identified the authors' first and last names in the researcher information table on the next page. **Names will be indexed and cited as shown on the proof, so these must be correct.**
- Any funding bodies have been acknowledged appropriately and included both in the paper and in the funder information table on the next page.
- All of the editor's queries are answered.
- Any necessary attachments, such as updated images or ESI files, are provided.

Translation errors can occur during conversion to typesetting systems so you need to read the whole proof. In particular please check tables, equations, numerical data, figures and graphics, and references carefully.

Please return your **final** corrections, where possible within **48 hours** of receipt following the instructions in the proof notification email. If you require more time, please notify us by email to materialsC@rsc.org.

Funding information

Providing accurate funding information will enable us to help you comply with your funders' reporting mandates. Clear acknowledgement of funder support is an important consideration in funding evaluation and can increase your chances of securing funding in the future.

We work closely with Crossref to make your research discoverable through the Funding Data search tool (<http://search.crossref.org/funding>). Funding Data provides a reliable way to track the impact of the work that funders support. Accurate funder information will also help us (i) identify articles that are mandated to be deposited in **PubMed Central (PMC)** and deposit these on your behalf, and (ii) identify articles funded as part of the **CHORUS** initiative and display the Accepted Manuscript on our web site after an embargo period of 12 months.

Further information can be found on our webpage (<http://rsc.li/funding-info>).

What we do with funding information

We have combined the information you gave us on submission with the information in your acknowledgements. This will help ensure the funding information is as complete as possible and matches funders listed in the Crossref Funder Registry.

If a funding organisation you included in your acknowledgements or on submission of your article is not currently listed in the registry it will not appear in the table on this page. We can only deposit data if funders are already listed in the Crossref Funder Registry, but we will pass all funding information on to Crossref so that additional funders can be included in future.

Please check your funding information

The table below contains the information we will share with Crossref so that your article can be found *via* the Funding Data search tool. **Please check that the funder names and grant numbers in the table are correct and indicate if any changes are necessary to the Acknowledgements text.**

Funder name	Funder's main country of origin	Funder ID (for RSC use only)	Award/grant number
Ministerio de Ciencia e Innovación	Spain	501100004837	GENESIS PID2019-111682RB-I00 and through the "Severo Ochoa" Programme
H2020 Marie Skłodowska-Curie Actions	European Union	100010665	No. 811284 (UHMob)
Generalitat de Catalunya	Spain	501100002809	2017-SGR-918
Fonds De La Recherche Scientifique - FNRS	Belgium	501100002661	2.5020.11
Fédération Wallonie-Bruxelles	Belgium	501100002910	20061
Università di Bologna	Italy	501100005969	Unassigned

Q1

Researcher information

Please check that the researcher information in the table below is correct, including the spelling and formatting of all author names, and that the authors' first, middle and last names have been correctly identified. **Names will be indexed and cited as shown on the proof, so these must be correct.**

If any authors have ORCID or ResearcherID details that are not listed below, please provide these with your proof corrections. Please ensure that the ORCID and ResearcherID details listed below have been assigned to the correct author. Authors should have their own unique ORCID iD and should not use another researcher's, as errors will delay publication.

Please also update your account on our online [manuscript submission system](#) to add your ORCID details, which will then be automatically included in all future submissions. See [here](#) for step-by-step instructions and more information on author identifiers.

First (given) and middle name(s)	Last (family) name(s)	ResearcherID	ORCID iD
Lamiaa	Fijahi		0000-0002-6185-1971
Tommaso	Salzillo	B-7912-2019	0000-0002-9737-2809
Adrián	Tamayo		
Marco	Bardini		

Christian	Ruzié		
Claudio	Quarti	O-9063-2017	0000-0002-5488-1216
David	Beljonne		0000-0001-5082-9990
Simone	d'Agostino		0000-0003-3065-5860
Yves	Geerts		
Marta	Mas-Torrent		0000-0002-1586-005X

Queries for the attention of the authors

Journal: **Journal of Materials Chemistry C**

Paper: **d2tc00655c**

Title: **Charge transfer complexes of a benzothienobenzothiophene derivative and their implementation as active layer in solution-processed thin film organic field-effect transistors**

For your information: You can cite this article before you receive notification of the page numbers by using the following format: (authors), J. Mater. Chem. C, (year), DOI: 10.1039/d2tc00655c.

Editor's queries are marked on your proof like this **Q1**, **Q2**, etc. and for your convenience line numbers are indicated like this 5, 10, 15, ...

Please ensure that all queries are answered when returning your proof corrections so that publication of your article is not delayed.

Query reference	Query	Remarks
Q1	Funder details have been incorporated in the funder table using information provided in the article text. Please check that the funder information in the table is correct.	
Q2	Have all of the author names been spelled and formatted correctly? Names will be indexed and cited as shown on the proof, so these must be correct. No late corrections can be made.	
Q3	Please check that the inserted CCDC numbers are correct.	
Q4	Are all of the author addresses and affiliation links correct?	
Q5	Please note that a conflict of interest statement is required for all manuscripts. Please read our policy on Conflicts of interest (http://rsc.li/conflicts) and provide a statement with your proof corrections. If no conflicts exist, please state that "There are no conflicts to declare".	
Q6	Have all of the funders of your work been fully and accurately acknowledged?	

Charge transfer complexes of a
benzothienobenzothiophene derivative and their
implementation as active layer in solution-
processed thin film organic field-effect
transistors†Lamiaa Fijahi,^a Tommaso Salzillo,^b ‡*^a Adrián Tamayo,^a Marco Bardini,^b
Christian Ruzié,^c Claudio Quarti,^b David Beljonne,^b *^b Simone d'Agostino,^b *^d
Yves Geerts^c and Marta Mas-Torrent^b *^a

Herein, we report on the synthesis and structural characterization of novel charge transfer (CT) complexes of the benzothienobenzothiophene derivative C₈O-BTBT-OC₈ with the series of F_xTCNQ derivatives (x = 2, 4). The degree of charge transfer and HOMO–LUMO gap energies were evaluated by spectroscopic means and by DFT calculations. Thin films of the (C₈O-BTBT-OC₈)(F₄TCNQ) complex were prepared by a simple solution shearing technique and by blending the active materials with polystyrene. X-Ray diffraction and IR/Raman spectroscopy techniques were instrumental for the structural identification of the films, which belonged to the same phase as the resolved single crystal. The films were implemented as an active layer in organic field-effect transistor (OFET) devices, which exhibited an n-type behavior in ambient conditions in agreement with the theoretical calculations.

Received 16th February 2022,
Accepted 13th April 2022

DOI: 10.1039/d2tc00655c

rsc.li/materials-c

Introduction

Organic charge-transfer (CT) complexes are two component systems formed by an electron Donor (D) and an electron Acceptor (A) unit with a specific stoichiometry. These binary systems are characterised by a charge transfer state with a certain ionicity (ρ) that can range from neutral ($\rho = 0$) to the fully ionised form ($\rho = 1$). The degree of charge transfer depends on the chemical structure of their constituents, but also on the overlap between their frontier molecular orbitals. Typically, D/A CT single crystals organise in either segregated

(*i.e.*, –D–D–D– and A–A–A–) or mixed (*i.e.*, –D–A–D–A–) π -stacks. Both the packing and charge transfer degree importantly determine the resulting electrical properties, which can vary from insulator, semiconductor, and metallic to superconductor.^{1,2} For many decades CT complexes were intensively investigated in order to establish guidelines to design materials exhibiting high room-temperature mobility or superconductivity.³ However, in the more recent years, the focus has also been placed on the development of more technologically relevant applications deploying such CT complexes,^{4–6} including thermoelectrics,⁷ photoconductors,^{8,9} strain sensors,¹⁰ light detectors,¹¹ ferroelectrics¹² or organic field-effect transistors (OFETs), where CT complexes can act as organic metals^{13,14} or organic semiconductors.^{15,16}

The separate D or A units in a CT complex typically can act as unipolar (p and n, respectively) organic semiconductors when implemented in an OFET.^{17,18} However, when they co-crystallise together, they can exhibit completely different properties. Hence, significant efforts are being devoted on exploring the electrical performance of a variety of CT systems as active layers in OFETs. Nonetheless, these studies have been mainly restricted to prototypical single crystals or co-evaporated thin films, which are not desirable for practical applications.^{19–21} Indeed, the preparation of thin films of CT complexes over large areas employing solution-based techniques is highly

^a Institut de Ciència de Materials de Barcelona (ICMAB-CSIC), Campus de la UAB, 08193 Bellaterra, Barcelona, Spain. E-mail: mmas@icmab.es

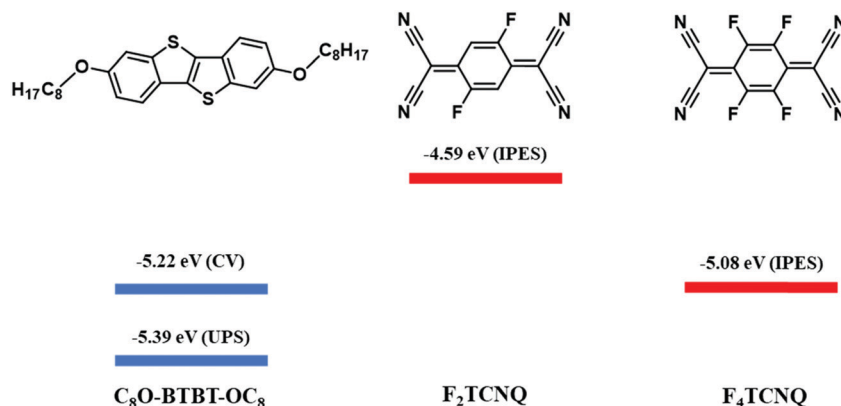
^b Laboratory for Chemistry of Novel Materials, University of Mons, 7000 Mons, Belgium. E-mail: David.Beljonne@umons.ac.be

^c International Solvay Institutes of Physics and Chemistry and Laboratoire de Chimie des Polymères, Faculté des Sciences, Université Libre de Bruxelles (ULB), CP 206/01, Boulevard du Triomphe, 1050, Brussels, Belgium

^d Chemistry Department “Giacomo Ciamician”, University of Bologna, Via F. Selmi 2, 40126 Bologna, Italy. E-mail: simone.dagostino2@unibo.it

† Electronic supplementary information (ESI) available. CCDC 2151123 and 2151124. For ESI and crystallographic data in CIF or other electronic format see <https://doi.org/10.1039/d2tc00655c>

‡ Current address: Dipartimento di Chimica Industriale “Toso Montanari”, Università di Bologna, Viale del Risorgimento 4, 40136 Bologna, Italy. E-mail: <https://tommaso.salzillo@unibo.it>



Scheme 1 Molecular structures of the donor (C_8O -BTBT- OC_8) and acceptor (F_2 TCNQ and F_4 TCNQ) compounds, and HOMO (blue) and LUMO (red) energy levels for C_8O -BTBT- OC_8 , F_2 TCNQ, and F_4 TCNQ.^{22,23} The LUMO levels of the acceptor molecules were estimated by Inverse Photoemission Spectroscopy (IPES). The HOMO levels of C_8O -BTBT- OC_8 estimated by Cyclic Voltammetry (CV) and Ultra-Violet Photoelectron Spectroscopy (UPS) are shown.

challenging since the solubility of the separate components in organic solvents is distinct to the one from the CT complex. Recently, we reported the fabrication of thin films of the CT complex dibenzotetrathiafulvalene-7,7,8,8-tetracyanoquinodimethane (DBTTF)(TCNQ) employing a solution shearing deposition technique.^{17,18} This was achieved by blending the CT complex with an insulating binding polymer to promote film processability and crystallinity.

Here, we report the preparation and characterisation of two novel CT crystals based on 2,7-bis(octyloxy)[1]benzothieno[3,2-*b*]benzothiophene (C_8O -BTBT- OC_8) and fluorinated 7,7,8,8-tetracyanoquinodimethane (*i.e.*, F_2 TCNQ and F_4 TCNQ) (Scheme 1). In both cases, the donor and acceptor molecules co-crystallise in a 1:1 stoichiometry forming stacks of alternating C_8O -BTBT- OC_8 and F_2 TCNQ or F_4 TCNQ. A low charge transfer degree is found for the CT complex based on F_2 TCNQ, whereas this value is increased with the more electron acceptor F_4 TCNQ derivative. Further, thin films of (C_8O -BTBT- OC_8)(F_4 TCNQ), corresponding to the same crystal phase as the single crystal one, were successfully prepared employing a high throughput solution-based deposition technique in ambient conditions. The films were characterised as active layer in OFETs giving an n-type behaviour.

Results and discussions

The BTBT derivative C_8O -BTBT- OC_8 (Scheme 1) has previously been reported as a highly promising p-type organic semiconductor.^{22,24} However, CT complexes with this derivative have never been reported before. CT complexes based on C_8O -BTBT- OC_8 with TCNQ, F_2 TCNQ and F_4 TCNQ were attempted to grow, although with the non-fluorinated acceptor no complex was formed. The later cannot be explained by the mismatch of the highest occupied molecular orbital (HOMO) of the donor with the lowest unoccupied molecular orbital (LUMO) of the acceptor,²⁵ since CT complexes with TCNQ have been reported

for other BTBT derivatives, with even deeper HOMO level.^{6,20,21,26–28}

Both CT complexes, (C_8O -BTBT- OC_8)(F_2 TCNQ) and (C_8O -BTBT- OC_8)(F_4 TCNQ), crystallize as isomorphous in the triclinic $P\bar{1}$ space group (see Table S1 for details and Fig. S1, ESI[†]), and feature extended stacks, running along the *a*-axis, in which molecules of the donor C_8O -BTBT- OC_8 alternate with the corresponding acceptor TCNQ-derivative in an $\cdots A \cdots D \cdots A \cdots D \cdots$ fashion (Fig. 1). Despite the different nature of the TCNQ acceptor, the interplanar distances (plane to centroid) between C_8O -BTBT- OC_8 and F_2 TCNQ or F_4 TCNQ are only slightly different, accounting for 3.3 Å and 3.2 Å, respectively, which are slightly shorter compared with CT complexes made of analog BTBT donor derivatives.^{26,27} In both cases, the indexing of the crystal faces revealed that the long crystal axis corresponds to the crystallographic [1 0 0] direction, and hence, the $\pi \cdots \pi$ stacking direction (Fig. S2 and S3, ESI[†]). Additionally, it is worth noting how both (C_8O -BTBT- OC_8)(F_2 TCNQ) and (C_8O -BTBT- OC_8)(F_4 TCNQ) display a remarked structural

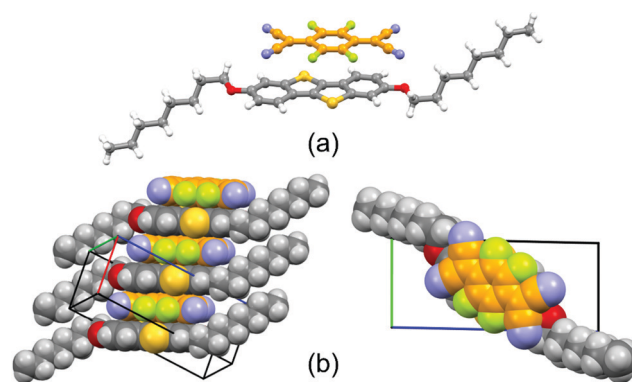


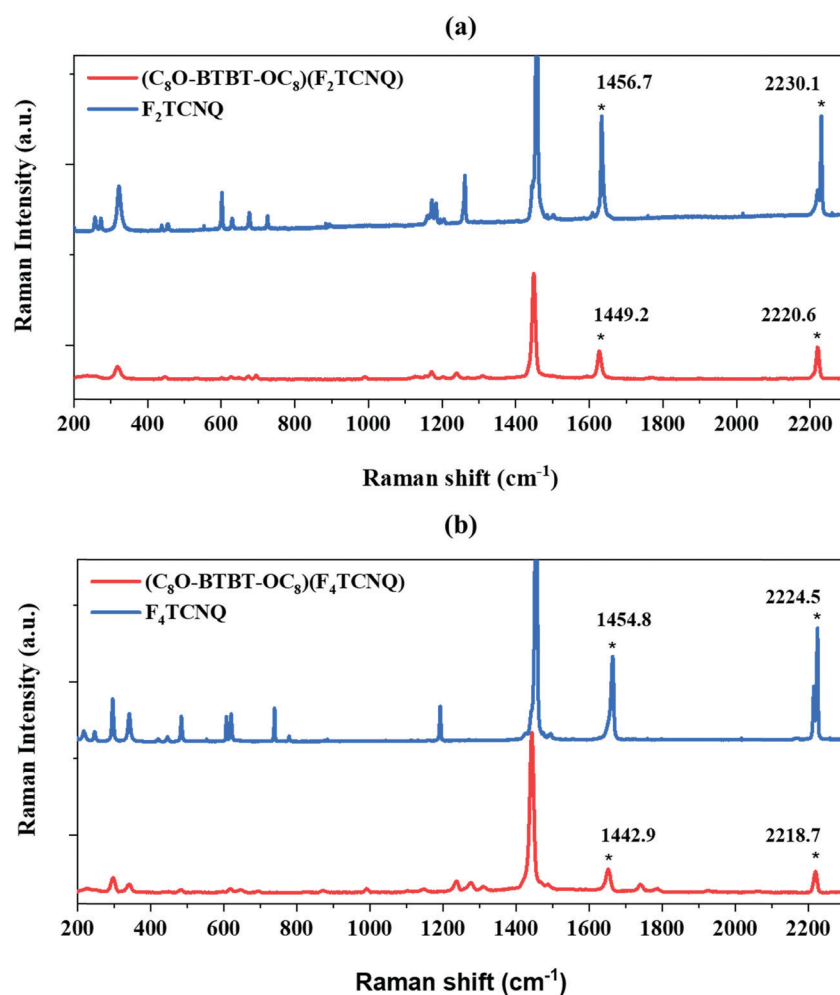
Fig. 1 Structural features of crystalline (C_8O -BTBT- OC_8)(F_4 TCNQ): (a) molecular structure of the CT complex as observed in its crystal, and (b) side and top views of the columnar stacking running along the *a*-axis. C-atoms of C_8O -BTBT- OC_8 and F_4 TCNQ molecules in grey and orange, respectively.

1 resemblance with other CT complexes made up of alkylated
benzothienobenzothiophene and TCNQ derivatives, which
were previously reported as promising candidates for the
development of OSCs.⁶

5 Raman and Infrared (IR) spectroscopy are non-destructive
techniques very useful for the characterisation of CT complexes
since it is well known that charge transfer interactions influ-
ence some vibrational modes of both donor and acceptor. Here,
10 Raman spectra of the single crystal CT complexes were com-
pared with the ones of the parent compounds (Fig. 2). For the
TCNQ derivatives two Raman active modes have been identified
to be sensitive^{29,30} to the degree of charge transferred from the
donor to the acceptor: the stretching of the C=C double bonds
15 of the central TCNQ core and the stretching of the periferic CN
groups. For the (C₈O-BTBT-OC₈)(F₂TCNQ) complex, the C=C
stretching shifts from 1456.7 to 1449.2 cm⁻¹ and the CN from
2230.1 to 2220.6 cm⁻¹, whereas in the case of (C₈O-BTBT-
OC₈)(F₄TCNQ) the C=C stretching shifts from 1454.8 to
20 1442.9 cm⁻¹ and the CN from 2224.5 to 2218.7 cm⁻¹. This
phenomena clearly indicates that a certain charge transfer

degree between the donor and the acceptor unit in both CT
complexes is occurring.

As previously mentioned, the ionicity (ρ) is a key parameter
in CT complexes. There are several experimental methods
which have been reported so far to determine ρ . The most
5 common one is using vibrational spectroscopy by checking the
shift of the so called “charge sensitive modes” as mentioned
above for the Raman spectra. However, it has been reported
that for mixed stack CT systems Raman spectroscopy is not the
best option for the determination of ρ due to its overestimation
10 because these modes are affected by the electron-phonon (or
electron-molecular vibration) coupling.^{30,31} Instead, IR modes
are more reliable. Again, for CT complexes based on F_xTCNQ,
the stretching of the CN periferic groups and C-C bonds have
been identified to be charge sensitive.²⁹ Considering that often
15 the CN group is influenced by the intermolecular interaction
network, the more reliable charge sensitive modes to estimate ρ
are the three ones attributed to the C-C bonds (Fig. 3a). These
modes appear at the following frequencies: ν_1 : 1577 cm⁻¹ and
1598 cm⁻¹; ν_2 : 1551 cm⁻¹ and 1550 cm⁻¹; ν_3 : 1396 cm⁻¹ and
20 1395 cm⁻¹, for F₂TCNQ and F₄TCNQ, respectively.^{18,29,30} The IR



55 Fig. 2 Raman spectra of (a) (C₈O-BTBT-OC₈)(F₂TCNQ) and (b) (C₈O-BTBT-OC₈)(F₄TCNQ). The C=C and CN charge sensitive modes are marked with an asterisk.

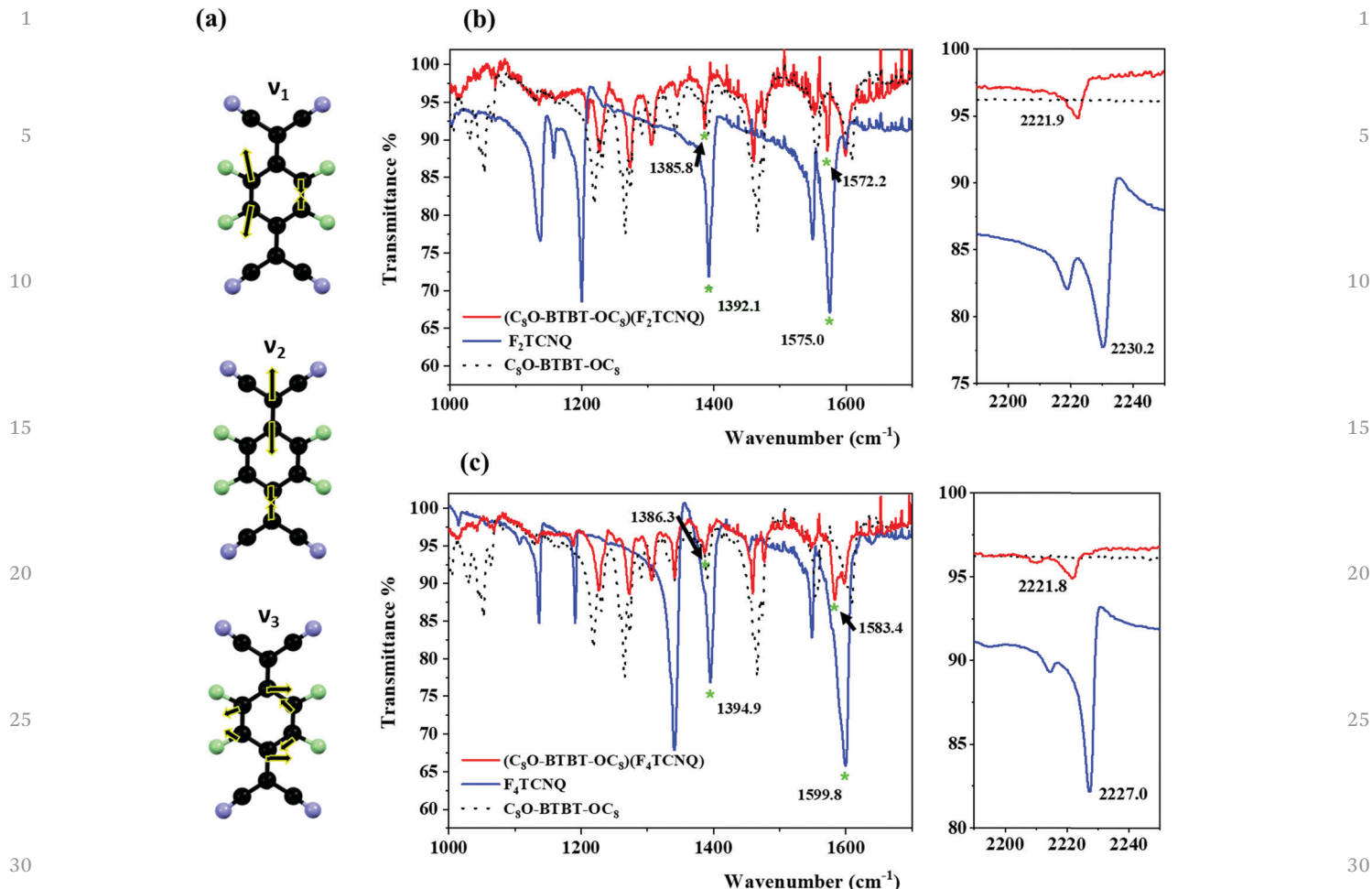


Fig. 3 (a) C–C charge sensitive modes for F₄TCNQ. (b) IR spectra of C₈O-BTBT-OC₈, F₂TCNQ and the corresponding CT complex. (c) IR spectra of C₈O-BTBT-OC₈, F₄TCNQ and the corresponding CT complex. The C–C charge sensitive modes are marked with an asterisk.

spectra of the prepared C₈O-BTBT-OC₈ CT complexes are shown in Fig. 3b and c together with the ones of the separate components. From the shift of the CN stretching (from 2230.2 to 2221.9 cm⁻¹ for (C₈O-BTBT-OC₈)(F₂TCNQ) and from 2227.0 to 2221.8 cm⁻¹ for (C₈O-BTBT-OC₈)(F₄TCNQ)) the CT interaction is confirmed in agreement with the Raman results. Furthermore, two of the three C–C charge sensitive modes are identified and marked on the IR spectrum (ν_1 : 1385.8 and 1386.3 cm⁻¹ and ν_3 : 1572.2 and 1583.4 cm⁻¹ for the F₂TCNQ and F₄TCNQ CT complex, respectively). The vibration ν_2 is probably too weak to be detected. Assuming a linear correlation between ρ and the frequency shifts, and knowing the frequencies of the modes ν_1 and ν_3 of the neutral (*i.e.*, F₂TCNQ and F₄TCNQ) and completely ionic (*i.e.*, K⁺F₂TCNQ and K⁺F₄TCNQ) species,²⁹ the ρ of the CT complexes was calculated. Accordingly, the estimated degree of ionicity was found to be 0.16 and 0.29 for (C₈O-BTBT-OC₈)(F₂TCNQ) and (C₈O-BTBT-OC₈)(F₄TCNQ), respectively. It is worth noting that ν_3 is very close to a vibration of the donor C₈O-BTBT-OC₈, which could generate certain underestimation of the degree of ionicity. These results show that a higher degree of CT is found with

the more electron acceptor F₄TCNQ (Scheme 1). Further, it is noticed that the ionicity in these derivatives is higher than the previously reported values found for BTBT and di-alkyl BTBT analogous CT complexes.^{25,26}

The optical HOMO–LUMO gap energies of the CT complexes were subsequently estimated by UV-Vis-NIR spectroscopy (Fig. S4, ESI[†]). This is realized according to the following equation:³²

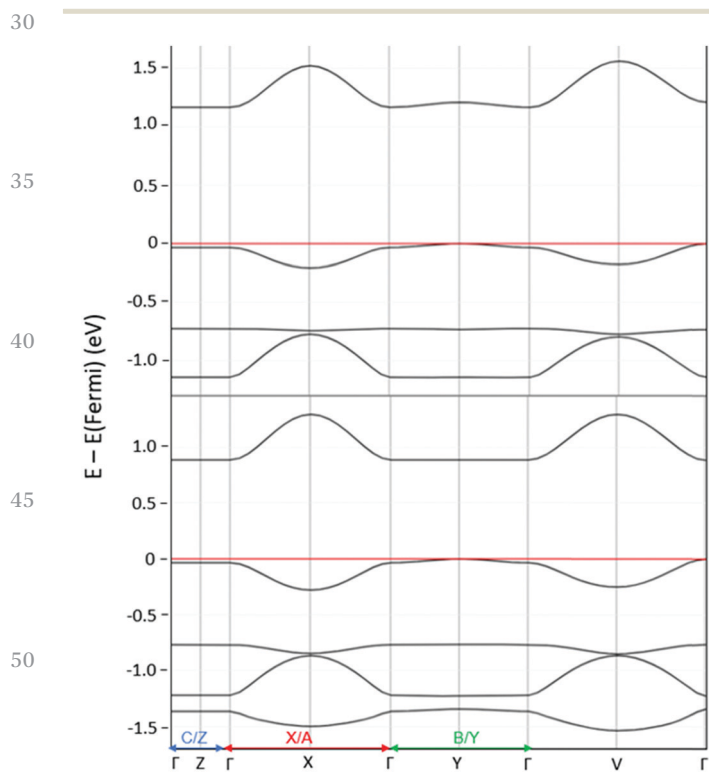
$$E_g = h \times \frac{c}{\lambda_{a.e.}} = \frac{1240}{\lambda_{a.e.}}$$

where E_g represents the optical band gap expressed in eV and $\lambda_{a.e.}$ denotes the absorption edge wavelength, expressed in nm, obtained from the offset wavelength derived from the lowest energy absorption band. The optical band gap for (C₈O-BTBT-OC₈)(F₂TCNQ) was estimated to be 0.96 eV, while for (C₈O-BTBT-OC₈)(F₄TCNQ) it was found to be lower, 0.80 eV.

Solid-state Density Functional Theory (DFT) electronic structure calculations were performed for the (C₈O-BTBT-OC₈)(F_xTCNQ) co-crystals using the hybrid B3LYP functional on the basis of the experimental single crystal X-ray structures. Mülliken population analysis yields an ionicity parameter ρ of 0.098 in (C₈O-BTBT-OC₈)(F₂TCNQ) and of 0.128 in (C₈O-BTBT-

1 OC₈(F₄TCNQ). We note that these values are larger than those
 2 obtained using a similar modeling protocol by Ashokan *et al.*²⁵
 3 ($\rho \sim 0.07$ in (C₈-BTBT-C₈)(F₂TCNQ) and (C₈-BTBT-
 4 C₈)(F₄TCNQ)) in the case of co-crystals involving the same
 5 acceptors but alkylated instead of alkoxyated BTBT derivatives
 6 as donors. Such a difference is associated with the stronger
 7 donor character of the C₈O-BTBT-OC₈ molecules induced by the
 8 electron pushing alkoxy moieties. The calculated ionicities are
 9 in good qualitative agreement with experiment (namely repro-
 10 duce the trend observed with increasing strength of the accep-
 11 tor), yet are slightly lower than the values of ~ 0.16 in (C₈O-
 12 BTBT-OC₈)(F₂TCNQ) and ~ 0.29 in (C₈O-BTBT-OC₈)(F₄TCNQ)
 13 inferred from the measured vibrational spectra. Such a discre-
 14 pancy is either due to the metric adopted to probe the degree of
 15 charge transfer or to the level of theory used (as pointed out in
 16 ref. 25 a proper description of the degree of ionicity in these
 17 crystals would require the use of optimally-tuned range sepa-
 18 rated functionals, currently not implemented), or a combi-
 19 nation of both.

20 The DFT calculated band structure of the (C₈O-BTBT-
 21 OC₈)(F₄₍₂₎TCNQ) co-crystals is reported in Fig. 4 and the
 22 extracted hole and electron effective masses collected in
 23 Table 1. Similar to the case of alkylated BTBT in ref. 25 we
 24 expect electrical transport in these co-crystals to be: (i) strongly
 25 anisotropic and predominantly one-dimensional, with much
 26 lower effective masses along the D:A stacking direction (see
 27 Table S2, ESI†); and (ii) dominated by electrons, with effective
 28 masses significantly smaller than the corresponding values for



55 Fig. 4 Band structures of (C₈O-BTBT-OC₈)(F₄TCNQ) (bottom) and (C₈O-
 56 BTBT-OC₈)(F₂TCNQ) (top). The direct lattice directions corresponding to
 57 the reciprocal lattice pathway are indicated on the X axis.

Table 1 Bandwidth along the stacking direction for the conduction band (CB) and valence band (VB) alongside the effective masses expressed with respect to the standard electron mass. Data from

Co-crystals	Bandwidth (meV)		Effective mass (m^*/m_0)	
	CB	VB	Electrons	Holes
(C ₈ -BTBT-C ₈)(TCNQ) ^a	280	82	1.0	3.1
(C ₈ -BTBT-C ₈)(F ₄ TCNQ) ^a	329	128	0.7	1.5
(C ₁₂ -BTBT-C ₁₂)(TCNQ) ^a	280	88	1.2	3.9
(C ₁₂ -BTBT-C ₁₂)(F ₄ TCNQ) ^a	316	110	1.1	3.6
(C ₈ O-BTBT-OC ₈)(F ₂ TCNQ) ^b	357	174	1.8	3.1
(C ₈ O-BTBT-OC ₈)(F ₄ TCNQ) ^b	408	244	1.4	2.0

^a Ref. 25. ^b This work.

holes. Additionally, the DFT calculated electronic bandgaps of 1.19 (0.89) eV in the F₂TCNQ (F₄TCNQ) doped co-crystal match reasonably well the measured optical gap of ~ 0.96 (~ 0.80) eV, though the comparison should be considered with care as electron-hole correlations are not included in the calculations.

Once characterised the single crystal CT complexes, we aimed at investigating their potential as organic semiconductors in OFETs. However, due to the difficulty of handling single crystals and their limited practical applicability, we focused on the preparation of thin films by a high throughput solution-based technique. The bar-assisted meniscus shearing (BAMS) technique was employed, which was previously used successfully to deposit a large family of organic semiconductors and a CT complex (Fig. 5a).^{18,33–38} This technique consists in placing a solution of the organic material between a bar and a heated substrate forming a confined meniscus and, immediately afterwards, displacing the substrate at a constant speed. It has also been shown that the use of polymer blends facilitates the processing of the films, the crystallisation of the semiconductor and the device stability.^{39–42}

After an optimisation process modifying the solution formulation (solvent and molecular weight and ratio of the polymer binder) and coating conditions (*i.e.*, temperature and speed), thin films of (C₈O-BTBT-OC₈)(F₂TCNQ) and (C₈O-BTBT-OC₈)(F₄TCNQ) were prepared using: (1) a 2 wt% solution of an equimolar ratio of C₈O-BTBT-OC₈ and F_xTCNQ in a mixture of chlorobenzene : benzonitrile (5 : 1), and (2) blending the solution prepared in (1) with a 2 wt% solution of polystyrene (PS) 280 kg mol⁻¹ in the same mixture of solvents in a ratio 4 : 1. The solutions were kept at high temperature to avoid precipitation of the materials. The deposition was performed at a speed of 2 mm s⁻¹ and keeping the substrate at 85 °C. Homogenous thin films of (C₈O-BTBT-OC₈)(F₄TCNQ) were successfully prepared. However, the films were not highly reproducibly fabricated with the CT (C₈O-BTBT-OC₈)(F₂TCNQ). Therefore, the following studies were focused only on thin films of (C₈O-BTBT-OC₈)(F₄TCNQ).

To assess the morphology and crystallinity of the semiconducting layer, optical polarised microscopy images of the thin films were taken and are shown in Fig. 5b. Both films (*i.e.*, with and without PS) show a similar polycrystalline morphology with small domains. A closer analysis by Atomic Force Microscopy (AFM) reveal that the films are formed by small stripe-shaped

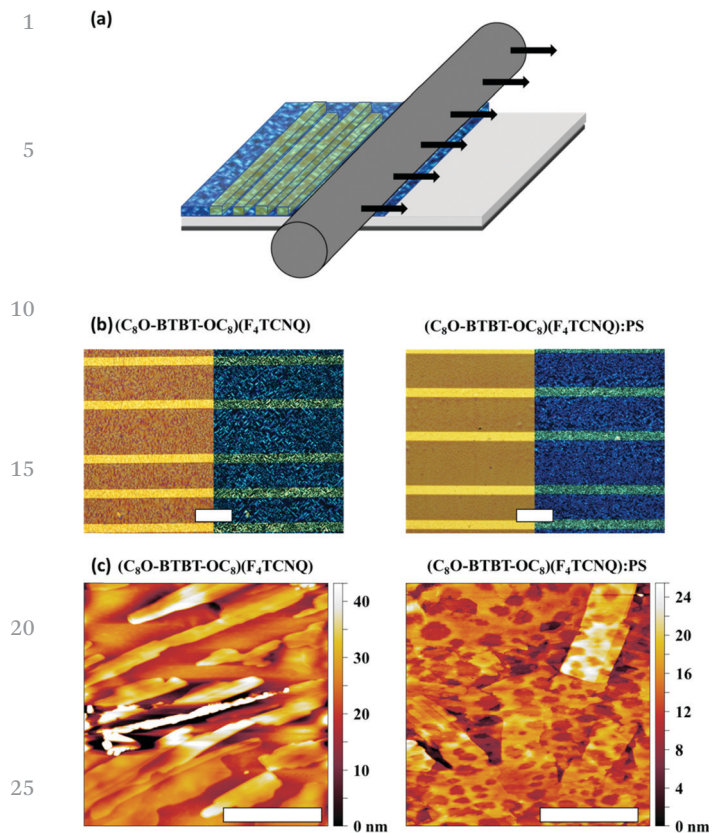


Fig. 5 (a) Schematic illustration of the BAMS technique. (b) Non polarized and polarized optical microscopy images with crossed polarizer/analyzer setup of $(C_8O-BTBT-OC_8)(F_4TCNQ)$ and $(C_8O-BTBT-OC_8)(F_4TCNQ):PS$ films. Scale bar: 100 μm . (c) AFM topography images of $(C_8O-BTBT-OC_8)(F_4TCNQ)$ and $(C_8O-BTBT-OC_8)(F_4TCNQ):PS$ films. Scale bar: 2 μm .

crystals without any preferential orientation along the surface (Fig. 5c). The thickness of $(C_8O-BTBT-OC_8)(F_4TCNQ)$ films was found to be (29.7 ± 8.4) nm with a root mean square roughness (R_{rms}) of 7.9 ± 6.3 nm, whereas $(C_8O-BTBT-OC_8)(F_4TCNQ):PS$ films were 23.8 ± 9.1 nm thick with a R_{rms} of 5.6 ± 2.1 nm.

In order to verify if the thin film corresponds to same crystal phase as the single crystal one described above, X-ray diffraction (XRD) along with spectroscopic characterization were carried out. Both XRD of the films with and without PS reveal two main peaks attributed to the (001) and (002) reflections that coincide with the single crystal structure (Fig. 6a). Moreover, the XRD data indicates that the crystals are oriented with the *ab* plane parallel to the substrate, and hence the stacking direction, that should coincide with the most favourable transport path, is parallel to the substrate.

Fig. 6b shows the Raman characterisation performed on thin films of $(C_8O-BTBT-OC_8)(F_4TCNQ)$ together with the one recorded for the single crystal for comparison. Interestingly, the shifts of the C-C and CN stretchings appear in the film at 1442.9 cm^{-1} and 2218.7 cm^{-1} , respectively, which perfectly match the ones previously found for the single crystal. The thin films were also inspected by Infrared Reflection-Absorption Spectroscopy (IRRAS). The frequencies of the C-C modes ν_1

and ν_3 are difficult to assign unambiguously (Fig. S5, ESI[†]). On the other hand, the CN stretching is clearly observed as in the single crystal at 2219 cm^{-1} (Fig. 6c), confirming the formation of the CT salt in the film.

Both $(C_8O-BTBT-OC_8)(F_4TCNQ)$ and $(C_8O-BTBT-OC_8)(F_4TCNQ):PS$ films were electrically characterized as active layers in OFETs under ambient conditions. Fig. 7 shows representative transfer characteristics (see Fig. S6 for the mobility profile and Fig. S7, ESI[†] for the output characteristics). All the devices exhibit n-type OFET behaviour, with an average electron mobility of $1.0 \pm 0.2 \times 10^{-3}$ $cm^2 V^{-1} s^{-1}$ and threshold voltage of 1.6 ± 6.4 V for the films with PS binder, while for pristine films the mobility was $1.4 \pm 0.3 \times 10^{-4}$ $cm^2 V^{-1} s^{-1}$ and the threshold voltage 11.3 ± 5.2 V (values averaged from three substrate coatings containing at least 12 devices each). Hence, the addition of the PS binder polymer increases the device mobility in one order of magnitude and reduces the threshold voltage. Such device improvement can be attributed to a decrease in the interfacial charge trap density produced by the passivation of the SiO_2 dielectric with PS.^{41,43,44} Further, the device electrical characteristics are consistent with the performed DFT calculations, which indicated that transport in this co-crystal should be dominated by electrons. It should be also noticed that the device mobility achieved with the blended films is of the same order as the values reported for analogous evaporated films based on different BTBT derivatives.^{16,21} Although CT complexes could in principle show ambipolar transport,^{18,45-48} complexes based on BTBT and fluorinated TCNQ typically have shown only n-type behavior.^{20,21,27,49} This has been partly attributed to the energy matching between the Fermi level of the Au electrodes and the frontier molecular orbitals of the CT system.^{16,20,21} Indeed, the energy levels $(C_8O-BTBT-OC_8)(F_4TCNQ)$ are mainly determined by the HOMO of the donor and the LUMO of the acceptor.¹⁶ Since the F_4TCNQ LUMO level is close the Au work-function (*i.e.*, the metal used for the source-drain contacts), the injection of electrons is more favourable in this device configuration.

Generally, n-channel OFETs suffer from air-instability because the presence of water and oxygen reduces the device performance. This particularly applies to thin film transistors, including F_4TCNQ . However, it has been claimed that two-component molecular compounds composed of TCNQ are much more stable due to the intermolecular CT interaction in the solid state.^{20,27} Importantly to highlight is that the devices were here prepared and measured completely under ambient conditions. Further, around 40% of the prepared devices based on $(C_8O-BTBT-OC_8)(F_4TCNQ):PS$ were still operating properly after 30 days stored in environmental conditions, although this percentage decreased to 20–25% for the non-blended films.

In conclusion, we prepared and characterised two new CT crystals based on the organic semiconductor $C_8O-BTBT-OC_8$, namely $(C_8O-BTBT-OC_8)(F_2TCNQ)$ and $(C_8O-BTBT-OC_8)(F_4TCNQ)$. Both systems crystallise in a 1:1 stoichiometry forming alternating stacks of $C_8O-BTBT-OC_8$ and F_2TCNQ or F_4TCNQ . The ionicity was estimated by spectroscopic means to be 0.16 for $(C_8O-BTBT-OC_8)(F_2TCNQ)$ and increased to 0.29 for

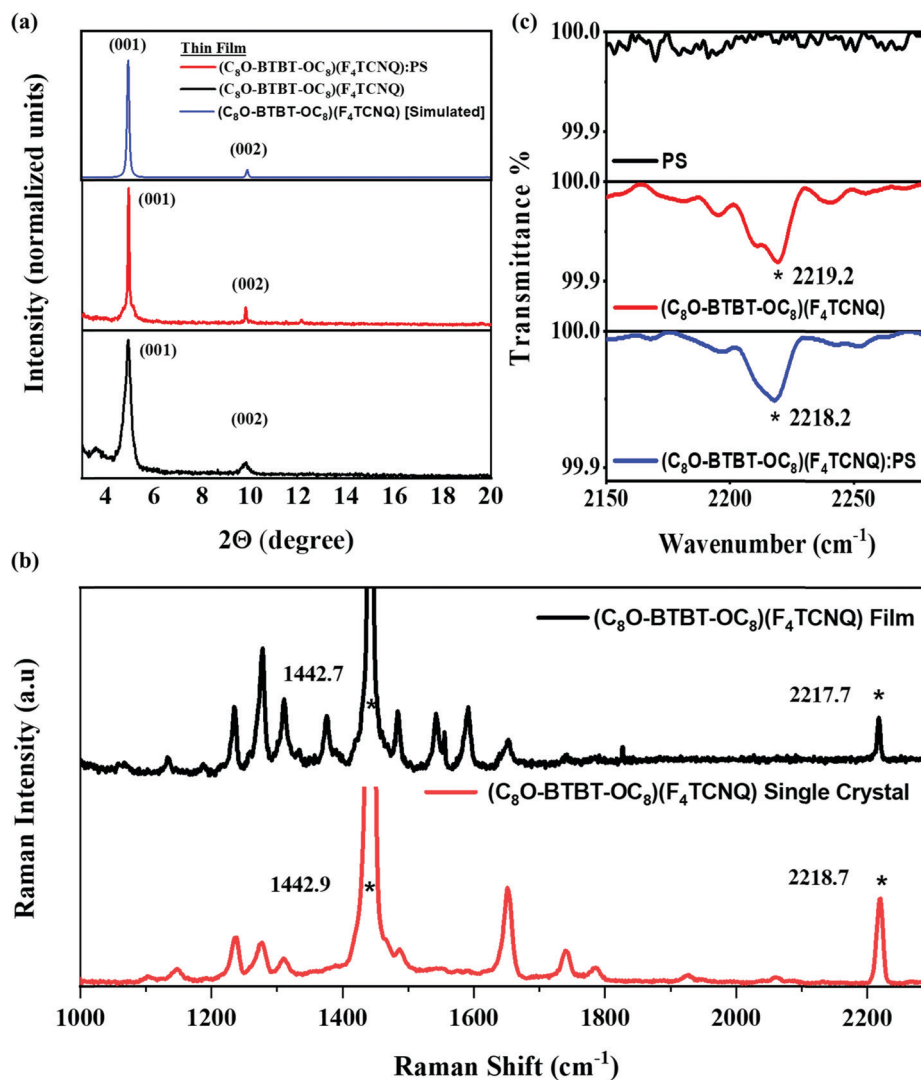


Fig. 6 (a) XRD diffractograms of thin films of (C₈O-BTBT-OC₈)(F₄TCNQ) and (C₈O-BTBT-OC₈)(F₄TCNQ):PS. (b) Raman spectra of a (C₈O-BTBT-OC₈)(F₄TCNQ) thin film and the one corresponding to the single crystal. (c) IRRAS spectra of (C₈O-BTBT-OC₈)(F₄TCNQ):PS, (C₈O-BTBT-OC₈)(F₄TCNQ) and PS thin films. The relevant charge sensitive modes are marked with an asterisk.

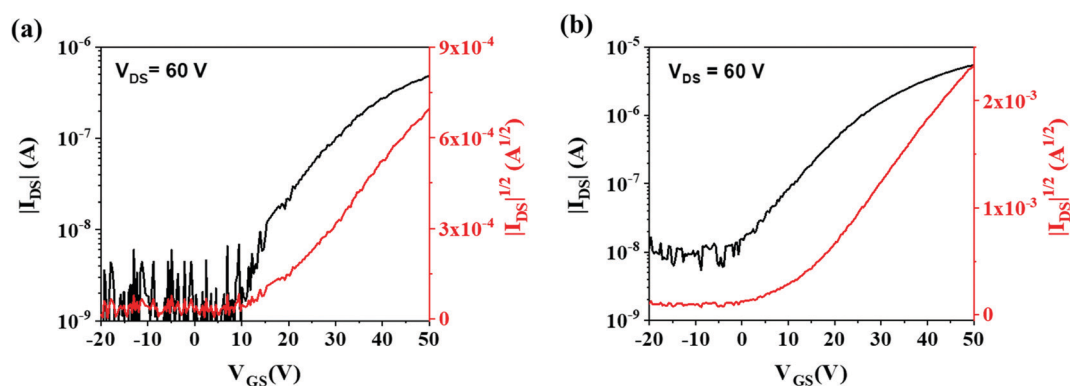


Fig. 7 Transfer characteristics of the OFETs based on (a) (C₈O-BTBT-OC₈)(F₄TCNQ) and (b) (C₈O-BTBT-OC₈)(F₄TCNQ):PS. The channel length is 150 μm and the width/length ratio is 100.

1 (C₈O-BTBT-OC₈)(F₄TCNQ). Similar results were found using
 DFT calculations, which showed the same tendency in which
 a higher charge transfer is occurring with the more electron
 acceptor unit F₄TCNQ. In addition, homogenous thin films
 5 based on the CT (C₈O-BTBT-OC₈)(F₄TCNQ) and (C₈O-BTBT-
 OC₈)(F₄TCNQ) blended with PS, were successfully prepared
 employing a solution-based technique compatible with roll-to-
 roll processes in ambient conditions. By a combination of XRD
 and spectroscopic techniques it was proved that the films are
 10 based on the same phase as the single crystal. Importantly, the
 films were implemented as active layers in OFETs, showing an
 n-type behaviour, in agreement with DFT calculations that
 pointed that transport in this co-crystal is dominated by
 electrons. This work shows that CT complexes are highly
 15 appealing materials for their unique tuneable electrical prop-
 erties and can, in addition, potentially have applicability in
 devices by finding suitable routes to process them as thin films
 deploying low-cost solution-based techniques.

20 Experimental section

Materials and methods

25 C₈O-BTBT-OC₈, synthesized by the procedure previously
 described.²² Polystyrene (PS) 280.000 kDa and 2,3,4,5,6-
 pentafluorothiophenol (PFBT) were purchased from Sigma-
 Aldrich and used without further purification. All the solvents
 (from Aldrich) were of spectroscopic grade.

Synthesis and crystal growth

30 CT complexes of C₈O-BTBT-OC₈/F_xTCNQ were prepared by
 dissolving an equimolar amount of C₈O-BTBT-OC₈ and F₂TCNQ
 or F₄TCNQ in the mixed solvent toluene : acetonitrile 5 : 1. The
 resulting solutions were heated at 80 °C for one hour to ensure
 35 the complete dissolution of the components; then, they were
 left to cool down in ambient conditions in the dark overnight
 slowly. The crystals were filtered and washed firstly with mother
 liquor and then with fresh solvent to remove residual parent
 components. The CT crystals appear as very thin dark needles,
 40 large 15–20 μm, and extended up to 3 mm.

Single crystal X-ray diffraction

45 Single-crystal data for (C₈O-BTBT-OC₈)(F₂TCNQ) and (C₈O-
 BTBT-OC₈)(F₄TCNQ) were collected at 200 K on an Oxford
 X'Calibur S CCD diffractometer equipped with a graphite
 monochromator (Mo-Kα radiation, λ = 0.71073 Å), and with a
 cryostat Oxford CryoStream800. The structures were solved by
 intrinsic phasing with SHELXT⁵⁰ and refined on F² by full-
 matrix least squares refinement with SHELXL⁵¹ implemented
 50 in the Olex2 software.⁵² All non-hydrogen atoms were refined
 anisotropically applying the rigid-body RIGU restraint.⁵³ H_{CH}
 atoms for all compounds were added in calculated positions
 and refined riding on their respective carbon atoms. In crystal-
 line (C₈O-BTBT-OC₈)(F₂TCNQ) the F₂TCNQ molecule was found
 55 to be disordered over two positions and refined to *ca.* 80/20 by
 adding a second free variable in the FVAR command line. Data

collection and refinement details are listed in Table S1 (ESI†).
 The Mercury program⁵⁴ was used to calculate intermolecular
 interactions and for molecular graphics. CCDC numbers
 2151123 and 2151124.†

Transistor fabrication and characterization

The bottom-gate/bottom-contact substrates employed for
 solution coating consisted of Si/SiO₂ substrates (200 nm SiO₂)
 from Si-Mat with photolithography patterned interdigitated
 electrodes of 4 nm of Cr and 40 nm of gold, deposited by
 thermal evaporation at deposition rates of 0.1–0.5 Å s⁻¹ and 1–5
 Å s⁻¹, respectively (Micro-Writer ML3 from Durham Magneto
 Optics). The channel lengths were 100 and 150 μm and the
 channel width/length ratio was always set to 100. The sub-
 strates were cleaned with acetone and isopropanol and then
 dried under nitrogen flow. Before the organic semiconductor
 deposition, the gold contacts were chemically modified. The
 substrates were cleaned using ultraviolet ozone cleaner for 25
 min and then they were immersed in a 15 mM solution of PFBT
 in isopropanol for 15 min. Finally, the substrates were rinsed
 20 with pure isopropanol and dried under a nitrogen flow. The
 (C₈O-BTBT-OC₈)(F₄TCNQ) and (C₈O-BTBT-OC₈)(F₄TCNQ):PS
 active layers were deposited by Bar-assisted meniscus Shearing
 (BAMS)^{33,35,38} using a home-designed instrument. The inks
 consisted of: (1) a 2 wt% solution of an equimolar ratio of
 25 C₈O-BTBT-OC₈ and F₄TCNQ in a mixture of chlorobenzene :
 benzonitrile (5 : 1), and (2) blending the solution prepared in
 (1) with a 2 wt% solution of polystyrene (PS) 280 kg mol⁻¹ in
 the same mixture of solvents in a ratio 4 : 1. The inks were heated at
 85 °C and, subsequently, deposited at 2 mm s⁻¹ and at a stage
 temperature of 85 °C.

Transistor measurements were carried out with an Agilent
 B1500A semiconductor device analyzer at ambient conditions.
 For all transfer measurements the V_{DS} were 10 V (linear) and
 60 V (saturation). The devices were characterized extracting the
 field-effect mobility in saturation regime, threshold voltage
 (V_{TH}) and on-off ratio. μ and V_{TH} was extracted using the
 following equations:

$$\mu^{\text{sat}} = \left(\frac{\partial \sqrt{I_{\text{DS}}}}{\partial V_{\text{GS}}} \right)^2 \frac{2L}{W} \cdot \frac{1}{C}$$

where *W* and *L* are the width and length of the channel,
 respectively, and *C* is the insulator capacitance per unit area
 (17.26 nF cm⁻²).

Spectroscopic measurements

Raman spectra were recorded using a Horiba XploRA PLUS
 spectrometer equipped with a suitable edge filter and coupled
 to an Olympus BX51 confocal microscope with 100× and 10×
 objectives, which allow for a lateral resolution lower than 1 μm
 with the higher magnification and a laser excitation wavelength
 of 532 nm.

For single crystal, infrared (IR) spectra were obtained in
 transmission mode with a Jasco 4700 Fourier transform (FTIR)
 spectrometer in the spectral range from 400–4000 cm⁻¹ with a

1 resolution of 1 cm^{-1} and 32 scans and absorption spectra, in
 the same configuration, were obtained from a Jasco V-780 UV/
 visible/NIR spectrophotometer. For both IR and UV-Vis-NIR
 measurements the powders of the pristine donor $\text{C}_8\text{O-BTBT-}$
 5 OC_8 , the acceptors F_2TCNQ and F_4TCNQ , and the crystals of the
 charge transfer complexes were dispersed in a 200 mg of
 spectroscopic grade KBr and used as pellet

For thin films characterization we used Infrared Reflection-
 Absorption Spectroscopy (IRRAS), an established analytical
 10 technique for the characterization of adsorbed matter and thin
 layers on metal surfaces. The spectra were recorded by using a
 Bruker Vertex 70 spectrometer with the PM50 module equipped
 with a liquid-nitrogen-cooled mercury-cadmium-telluride
 (MCT) photodetector and a permanently aligned Rock Solid
 15 interferometer. To reduce absorption due to water and carbon
 dioxide, the spectrometer was purged by fluxing nitrogen gas.
 The Bruker spectroscopy software OPUS, version 4.2, was used
 to operate the spectrometer.

20 Structural and morphological thin film characterizations

Optical microscope pictures were taken using an Olympus BX51
 equipped with polarizer and analyzer. The X-ray diffraction
 measurements were carried out with a D-5000 model Siemens
 25 diffractometer that used Cu K-alpha radiation 1.540560 \AA . AFM
 images were obtained using a Park NX10 system using PPP-
 NCHR tips (Nanosensors) in noncontact mode and applying
 adaptive scan rate to slow down scan speed at crystallite
 borders. Subsequent data analysis was done using the Gwyd-
 30 dion software.

Theoretical calculations

DFT calculations: solid-state DFT simulations were performed
 using the fully periodic CRYSTAL17 software package.^{55,56} All
 35 calculations, including band structure and density of states
 (DOS) used experimental atomic positions and lattice vectors
 retrieved from Cambridge Crystallographic Data Centre (CCDC)
 or from measurements described in previous sections. Reciprocal
 space sampling was performed using the Monkhorst-Pack
 40 scheme, with a k -point mesh in the first Brillouin Zone (program
 keyword SHRINK: X X X). The tolerances for Coulomb and
 exchange integral cutoffs were set to $\Delta E < 10^{-8}$ Hartree
 (program keyword TOLINTEG: 8 8 8 8 16). The energy conver-
 45 gence criterion for geometric optimizations was set to $\Delta E <$
 10^{-12} Hartree (program keyword TOLDEE: 12). The energy
 convergence criterion for frequency calculations was likewise
 set to $\Delta E < 10^{-12}$ Hartree. The Pople basis sets 6-31G*^{57,58} was
 utilized for all calculations. The exchange correlation func-
 50 tional Becke 3-parameter Lee-Yang-Parr (B3LYP)⁵⁹ was used
 for all calculations. The ionicity parameter ρ was estimated
 from a Mulliken population analysis⁶⁰ performed in the solid
 state using the Crystal17 package, while the effective masses
 were calculated by fitting the band structure along a given
 55 reciprocal space direction (and therefore a given crystallo-
 graphic direction) with a polynomial function.

Conflicts of interest

1
 Q5

Acknowledgements

This work was funded by European Union's Horizon 2020
 research and innovation programme under the Marie Skłodowska-Curie
 grant agreement No. 811284 (UHMob), the Spanish Ministry with the
 project GENESIS PID2019-111682RB-I00 and through the "Severo Ochoa"
 Programme for Centers of Excellence in R&D (FUNFUTURE CEX2019-000917-S),
 the Generalitat de Catalunya (2017-SGR-918) and the Consortium des
 Equipements de Calcul Intensif (CECI), funded by the Fonds de
 la Recherche Scientifique de Belgique (F.R.S. – FNRS) under
 grant no. 2.5020.11. A. T. acknowledges his FPU fellowship. A. T
 and L. F. are enrolled in the UAB Materials Science PhD
 program. Y. G. is thankful to the Belgian National Fund for
 Scientific Research (FNRS) for financial support through
 research projects, Pi-Fast No. T.0072.18, and 2D to 3D No.
 30489208. Financial supports from the French Community of
 Belgium (ARC No. 20061) is also acknowledged. DB is a FNRS
 research director, CQ is a FNRS research associate. S. D.
 acknowledges financial support from the University of Bologna
 (RFO-Scheme).

5
 10
 15
 20
 25
 Q6

References

- 1 H. Jiang, P. Hu, J. Ye, K. K. Zhang, Y. Long, W. Hu and C. Kloc, *J. Mater. Chem. C*, 2018, **6**, 1884–1902. 30
- 2 L. Sun, W. Zhu, F. Yang, B. Li, X. Ren, X. Zhang and W. Hu, *Phys. Chem. Chem. Phys.*, 2018, **20**, 6009–6023.
- 3 J. M. Williams, J. R. Ferraro and R. J. Thorn, *Organic Superconductors (Including Fullerenes). Synthesis, Structure, Properties, and Theory*, Prentice-Hall, United States, 1992. 35
- 4 K. P. Goetz, D. Vermeulen, M. E. Payne, C. Kloc, L. E. McNeil and O. D. Jurchescu, *J. Mater. Chem. C*, 2014, **2**, 3065–3076.
- 5 W. Wang, L. Luo, P. Sheng, J. Zhang and Q. Zhang, *Chem. – Eur. J.*, 2021, **27**, 464–490.
- 6 G. Liu, J. Liu, A. S. Dunn, P. Nadazdy, P. Siffalovic, R. Resel, M. Abbas, G. Wantz and Y. H. Geerts, *Cryst. Growth Des.*, 2021, **21**, 5231–5239. 40
- 7 K. Harada, M. Sumino, C. Adachi, S. Tanaka and K. Miyazaki, *Appl. Phys. Lett.*, 2010, **96**, 124.
- 8 H. Alves, R. M. Pinto and E. S. Maçôas, *Nat. Commun.*, 2013, **4**, 1842. 45
- 9 J. Tsutsumi, T. Yamada, H. Matsui, S. Haas and T. Hasegawa, *Phys. Rev. Lett.*, 2010, **105**, 226601.
- 10 E. Laukhina, R. Pfattner, L. R. Ferreras, S. Galli, M. Mas-Torrent, N. Masciocchi, V. Laukhin, C. Rovira and J. Veciana, *Adv. Mater.*, 2010, **22**, 977–981. 50
- 11 S. Ullbrich, B. Siegmund, A. Mischok, A. Hofacker, J. Benduhn, D. Spoltore and K. Vandewal, *J. Phys. Chem. Lett.*, 2017, **8**, 5621–5625.
- 12 A. S. Tayi, A. K. Shveyd, A. C. H. Sue, J. M. Szarko, B. S. Rolczynski, D. Cao, T. Jackson Kennedy, 55

- 1 A. A. Sarjeant, C. L. Stern, W. F. Paxton, W. Wu, S. K. Dey, A. C. Fahrenbach, J. R. Guest, H. Mohseni, L. X. Chen, K. L. Wang, J. Fraser Stoddart and S. I. Stupp, *Nature*, 2012, **488**, 485–489.
- 5 13 R. Pfattner, C. Rovira and M. Mas-Torrent, *Phys. Chem. Chem. Phys.*, 2014, **17**, 26545–26552.
- 14 T. Uekusa, R. Sato, D. Yoo, T. Kawamoto and T. Mori, *ACS Appl. Mater. Interfaces*, 2020, **12**, 24174–24183.
- 15 H. Di, Wu, F. X. Wang, Y. Xiao and G. B. Pan, *J. Mater. Chem. C*, 2013, **1**, 2286–2289.
- 10 16 T. Higashino, M. Dogishi, T. Kadoya, R. Sato, T. Kawamoto and T. Mori, *J. Mater. Chem. C*, 2016, **4**, 5981–5987.
- 17 M. Mas-Torrent, M. Durkut, P. Hadley, X. Ribas and C. Rovira, *J. Am. Chem. Soc.*, 2004, **126**, 984–985.
- 15 18 T. Salzillo, A. Campos and M. Mas-Torrent, *J. Mater. Chem. C*, 2019, **7**, 10257–10263.
- 19 K. P. Goetz, H. F. Iqbal, E. G. Bittle, C. A. Hacker, S. Pookpanratana and O. D. Jurchescu, *Mater. Horizons*, 2022, **9**, 271–280.
- 20 20 Y. Shibata, J. Tsutsumi, S. Matsuoka, K. Matsubara, Y. Yoshida, M. Chikamatsu and T. Hasegawa, *Appl. Phys. Lett.*, 2015, **106**, 143303.
- 21 R. Sato, M. Dogishi, T. Higashino, T. Kadoya, T. Kawamoto and T. Mori, *J. Phys. Chem. C*, 2017, **121**, 6561–6568.
- 25 22 C. Ruzić, J. Karpinska, A. Laurent, L. Sanguinet, S. Hunter, T. D. Anthopoulos, V. Lemaure, J. Cornil, A. R. Kennedy, O. Fenwick, P. Samori, G. Schweicher, B. Chattopadhyay and Y. H. Geerts, *J. Mater. Chem. C*, 2016, **4**, 4863–4879.
- 23 K. Kanai, K. Akaike, K. Koyasu, K. Sakai, T. Nishi, Y. Kamizuru, T. Nishi, Y. Ouchi and K. Seki, *Appl. Phys. A: Mater. Sci. Process.*, 2009, **95**, 309–313.
- 30 24 T. Salzillo, A. Campos, A. Babuji, R. Santiago, S. T. Bromley, C. Ocal, E. Barrena, R. Jouclas, C. Ruzić, G. Schweicher, Y. H. Geerts and M. Mas-Torrent, *Adv. Funct. Mater.*, 2020, **30**, 2006115.
- 35 25 A. Ashokan, C. Hanson, N. Corbin, J. L. Brédas and V. Coropceanu, *Mater. Chem. Front.*, 2020, **4**, 3623–3631.
- 26 N. Castagnetti, A. Girlando, M. Masino, C. Rizzoli and C. Rovira, *Cryst. Growth Des.*, 2017, **17**, 6255–6261.
- 40 27 H. Koike, J. Tsutsumi, S. Matsuoka, K. Sato, T. Hasegawa and K. Kanai, *Org. Electron.*, 2016, **39**, 184–190.
- 28 H. Méndez, G. Heimel, A. Opitz, K. Sauer, P. Barkowski, M. Oehzelt, J. Soeda, T. Okamoto, J. Takeya, J. B. Arlin, J. Y. Balandier, Y. Geerts, N. Koch and I. Salzmann, *Angew. Chem., Int. Ed.*, 2013, **52**, 7751–7755.
- 45 29 T. Salzillo, M. Masino, G. Kociok-Köhn, D. Di Nuzzo, E. Venuti, R. G. Della Valle, D. Vanossi, C. Fontanesi, A. Girlando, A. Brillante and E. Da Como, *Cryst. Growth Des.*, 2016, **16**, 3028–3036.
- 50 30 T. Salzillo, R. G. Della Valle, E. Venuti, G. Kociok-Köhn, M. Masino, A. Girlando and A. Brillante, *J. Cryst. Growth*, 2019, **516**, 45–50.
- 31 M. Masino, T. Salzillo, A. Brillante, R. G. Della Valle, E. Venuti and A. Girlando, *Adv. Electron. Mater.*, 2020, **6**, 2000208.
- 32 X. Sun, Y. Liu, S. Chen, W. Qiu, G. Yu, Y. Ma, T. Qi, H. Zhang, X. Xu and D. Zhu, *Adv. Funct. Mater.*, 2006, **16**, 917–925.
- 33 F. G. del Pozo, S. Fabiano, R. Pfattner, S. Georgakopoulos, S. Galindo, X. Liu, S. Braun, M. Fahlman, J. Veciana, C. Rovira, X. Crispin, M. Berggren and M. Mas-Torrent, *Adv. Funct. Mater.*, 2016, **26**, 2379–2386.
- 34 T. Salzillo, N. Montes, R. Pfattner and M. Mas-Torrent, *J. Mater. Chem. C*, 2020, **8**, 15361–15367.
- 35 I. Temiño, F. G. Del Pozo, M. R. Ajayakumar, S. Galindo, J. Puigdollers and M. Mas-Torrent, *Adv. Mater. Technol.*, 2016, **1**, 1600090.
- 36 S. Georgakopoulos, F. G. del Pozo and M. Mas-Torrent, *J. Mater. Chem. C*, 2015, **3**, 12199–12202.
- 37 L. Pandolfi, A. Giunchi, A. Rivalta, S. D'Agostino, R. G. Della Valle, M. Mas-Torrent, M. Lanzi, E. Venuti and T. Salzillo, *J. Mater. Chem. C*, 2021, **9**, 10865–10874.
- 38 S. Galindo, A. Tamayo, F. Leonardi and M. Mas-Torrent, *Adv. Funct. Mater.*, 2017, **27**, 1700526.
- 39 S. Riera-Galindo, F. Leonardi, R. Pfattner and M. Mas-Torrent, *Adv. Mater. Technol.*, 2019, **4**, 1900104.
- 40 Q. Zhang, F. Leonardi, S. Casalini, I. Temiño and M. Mas-Torrent, *Sci. Rep.*, 2016, **6**, 39623.
- 41 A. Campos, S. Riera-Galindo, J. Puigdollers and M. Mas-Torrent, *ACS Appl. Mater. Interfaces*, 2018, **10**, 15952–15961.
- 25 42 A. Tamayo, S. Hofer, T. Salzillo, C. Ruzić, G. Schweicher, R. Resel and M. Mas-Torrent, *J. Mater. Chem. C*, 2021, **9**, 7186–7193.
- 43 A. F. Paterson, N. D. Treat, W. Zhang, Z. Fei, G. Wyatt-Moon, H. Faber, G. Vourlias, P. A. Patsalas, O. Solomeshch, N. Tessler, M. Heeney and T. D. Anthopoulos, *Adv. Mater.*, 2016, **28**, 7791–7798.
- 30 44 K. Zhao, O. Wodo, D. Ren, H. U. Khan, M. R. Niazi, H. Hu, M. Abdelsamie, R. Li, E. Q. Li, L. Yu, B. Yan, M. M. Payne, J. Smith, J. E. Anthony, T. D. Anthopoulos, S. T. Thoroddsen, B. Ganapathysubramanian and A. Amassian, *Adv. Funct. Mater.*, 2016, **26**, 1737–1746.
- 35 45 D. Vermeulen, L. Y. Zhu, K. P. Goetz, P. Hu, H. Jiang, C. S. Day, O. D. Jurchescu, V. Coropceanu, C. Kloc and L. E. McNeil, *J. Phys. Chem. C*, 2014, **118**, 24688–24696.
- 40 46 K. P. Goetz, J. Tsutsumi, S. Pookpanratana, J. Chen, N. S. Corbin, R. K. Behera, V. Coropceanu, C. A. Richter, C. A. Hacker, T. Hasegawa and O. D. Jurchescu, *Adv. Electron. Mater.*, 2016, **2**, 1600203.
- 47 Y. Qin, C. Cheng, H. Geng, C. Wang, W. Hu, W. Xu, Z. Shuai and D. Zhu, *Phys. Chem. Chem. Phys.*, 2016, **18**, 14094–14103.
- 48 J. Zhang, H. Geng, T. S. Virk, Y. Zhao, J. Tan, C. A. Di, W. Xu, K. Singh, W. Hu, Z. Shuai, Y. Liu and D. Zhu, *Adv. Mater.*, 2012, **24**, 2603–2607.
- 50 49 J. Tsutsumi, S. Matsuoka, S. Inoue, H. Minemawari, T. Yamada and T. Hasegawa, *J. Mater. Chem. C*, 2015, **3**, 1976–1981.
- 50 G. M. Sheldrick, *Acta Crystallogr., Sect. A: Found. Crystallogr.*, 2015, **71**, 3–8.

- 1 51 G. M. Sheldrick, *Acta Crystallogr., Sect. C: Struct. Chem.*, 2015, **71**, 3–8.
- 52 O. V. Dolomanov, L. J. Bourhis, R. J. Gildea, J. A. K. Howard and H. Puschmann, *J. Appl. Crystallogr.*, 2009, **42**, 339–341.
- 5 53 A. Thorn, B. Dittrich and G. M. Sheldrick, *Acta Crystallogr., Sect. A: Found. Crystallogr.*, 2012, **68**, 448–451.
- 54 C. F. Macrae, I. J. Bruno, J. A. Chisholm, P. R. Edgington, P. McCabe, E. Pidcock, L. Rodriguez-Monge, R. Taylor, J. Van De Streek and P. A. Wood, *J. Appl. Crystallogr.*, 2008, **41**, 466–470.
- 10 55 R. Dovesi, A. Erba, R. Orlando, C. M. Zicovich-Wilson, B. Civalleri, L. Maschio, M. Rérat, S. Casassa, J. Baima, S. Salustro and B. Kirtman, *Wiley Interdiscip. Rev.: Comput. Mol. Sci.*, 2018, **8**, e1360.
- 56 A. Erba, J. Baima, I. Bush, R. Orlando and R. Dovesi, *J. Chem. Theory Comput.*, 2017, **13**, 5019–5027.
- 57 W. J. Hehre, R. Ditchfield and J. A. Pople, *J. Chem. Phys.*, 1972, **56**, 2257.
- 58 M. M. Francl, W. J. Pietro, W. J. Hehre, J. S. Binkley, M. S. Gordon, D. J. DeFrees and J. A. Pople, *J. Chem. Phys.*, 1982, **77**, 3654–3665.
- 59 A. D. Becke, *Phys. Rev. A: At., Mol., Opt. Phys.*, 1988, **38**, 3098–3100.
- 60 R. S. Mulliken, *J. Chem. Phys.*, 1955, **23**, 1833.

15

15

20

20

25

25

30

30

35

35

40

40

45

45

50

50

55

55